WEDNESDAY SLIDE CONFERENCE 2016-2017

C o n f e r e n c e 23

19 April 2017

George A. Parker, DVM, PhD, DACVP, DABT, FIATP
Senior Scientific Director, Global Pathology
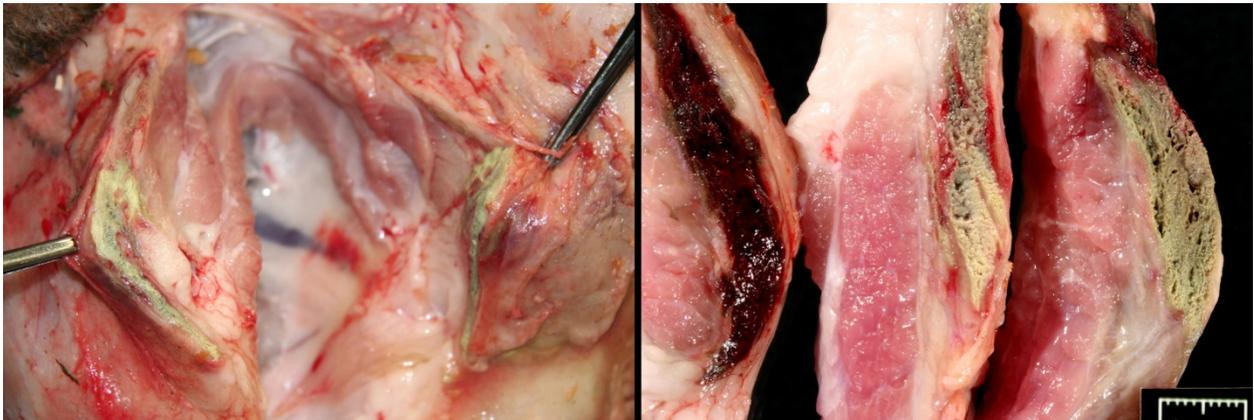Charles River Laboratories

---

CASE I: TAMU-02 2013 (JPC 4033348).

Signalment: Four-month-old Hampshire ewe (*Ovis aries*).

History: One of a number of young meat sheep showing neurological signs and hyperthermia. This sheep progressed through phases of straight legs, muscle fasciculations, and recumbency. A neurological examination revealed cranial nerves normal, mentation normal, recumbency, good muscle tone, head turn to left, normal to increased muscle tone. Localized to cervical spinal cord. This sheep was treated with flunixin and antibiotics with no response by owner.

Gross Pathology: Bilaterally the superficial pectoralis muscle is green-black, dry, and firm with surrounding red tissue in an oval area measuring 8 x 5 x 1cm on the right and 7 x 6 x 1cm on the left (Figs1,2.: severe,

Skeletal muscle, sheep. The superficial pectoralis muscle bilaterally contains large areas of dry-greenish black necrotic muscle. (Photo courtesy of: Department of Veterinary Pathobiology, College of Veterinary Medicine, Texas A&M University, College Station, TX).

Skeletal muscle, sheep. The left quadriceps and the left lateral head of the triceps are irregularly pale pink to gray, evidence of myodegeneration and necrosis. (Photo courtesy of: Department of Veterinary Pathobiology, College of Veterinary Medicine, Texas A&M University, College Station, TX).

myonecrosis and hemorrhage). The left quadriceps and the left lateral head of the triceps are irregularly pale pink to gray (Fig3.: myodegeneration/myonecrosis).

Numerous *Hemonchus* and *Trichostrongyles* are in the abomasum.

Laboratory results: No monensin or lasalocid in rumen contents
Feed analysis: 3.4% lasalocid (this 10,000 times the legal limit of 30g/ton, 33mg/kg, 33ppm)

Histopathologic Description: Longitudinal and cross sections of triceps muscle are examined. On cross section, round, large sometimes hyalinized, hypereosinophilic or flocculant fibers are seen with central, large nuclei. Some fibers remain as aggregates of activated satellite cells in a shrunken endomysium. On longitudinal section, swollen, hyalinized, broken, flocculent fibers with myocyte nuclear loss and contraction bands are prominent. Satellite cells are activated and proliferating with a large vesiculate chromatin and blue-grey cytoplasm. Macrophages and small clusters of degenerate neutrophils enter pockets of

broken fibers. Capillaries are lined by endothelial cells with hypertrophied nuclei.

Contributor's Morphologic Diagnosis: Subacute, monophasic myopathy with severe myofiber necrosis and satellite cell activation and early regeneration.

Contributor's Comment: The section shows a nice monophasic toxic myopathy. Ionophores are added to feeds for growth promotion and as a coccidiostat.[6,9] However, if toxic doses are achieved, they permit free cationic movement, especially calcium into myocytes and necrosis. Monogastrics such as the horse and dog are more susceptible.

This breeder had been having a chronic, sporadic, neurologic problem in the flock of show sheep. It affected sheep taken off pastured and "pushed" nutritionally for the show season. Upon opening this ewe, it was obvious that a myopathy was the problem, and given the history, we analyzed the rumen content (negative for ionophores additives), and then, the feed from the bag used to fed these ewes was tested (toxic levels of lasalocid). The levels of lasalocid the feed were extremely high, and it is presumed a pocket of unmixed, lasalocid

Abomasum, sheep: Numerous Haemonchus adults are attached to the mucosa. Photo courtesy of: Department of Veterinary Pathobiology, College of Veterinary Medicine, Texas A&M University, College Station, TX).

salt was included in the test sample. In some reports[2] and in this contributor's experience, once the ionophore is over a certain concentration, these additives are unpalatable, and animals refuse the feed rather than consume myotoxic levels. Unfortunately, toxicity studies are based on bolus feedings.[1,4]

In spontaneous, ionophore (usually monensin) intoxications of sheep[2,7,8,9,10] display an acute onset of signs of anorexia, dyspnea, muscle weakness, ataxia, a stiff gait and deaths follow feed changes. Firm or atrophic rear limb muscles are sometimes reported. A variety of autopsy lesions are reported including: cavitary effusions, pale-streaked hearts, diarrhea and pale-streaked skeletal muscles especially semi-membranosus and semitendinosus. While some acute gastrointestinal lesions are reported, consistent macroscopic and/or histologic lesions are in cardiac and skeletal muscles. In ovine monensin toxicity studies[1,4], it was commented that acute myopathies were not visible in H&E-stained sections, but that lesions were demonstrable

Skeletal muscle, sheep. Two sections of skeletal muscle from the triceps are submitted. The larger section on left shows muscle fibers in cross section; the smaller section on the right demonstrates fibers in longitudinal section. This is an excellent way to process muscle sections as many changes cannot be appreciated in cross section. (HE, 5X)
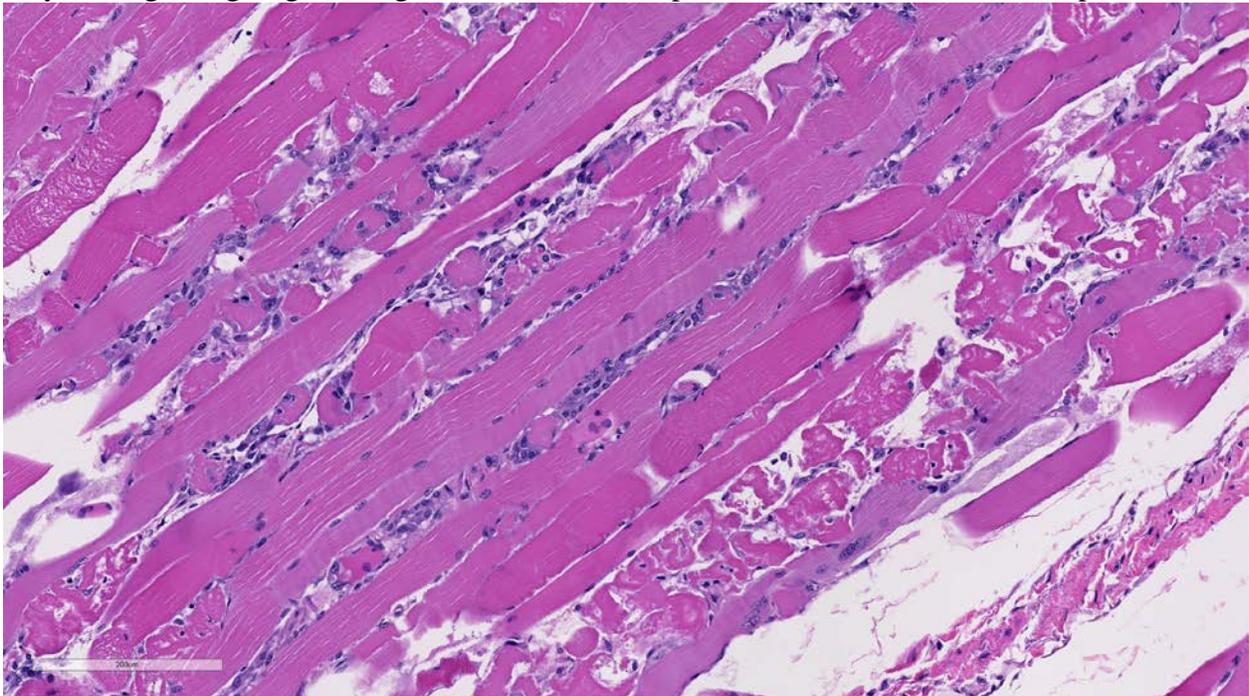
using electron microscopy. Early ultra-structure changes include mitochondrial swelling and myofibrillar disarray. Chronic histologic lesions include atrophy, fibrosis, and calcification. The severity of the present case is impressive, and the minimal cardiac lesion is unexplained. Is it possible that hypoxia from hemonchosis-exacerbated lesions?

Finally, many ionophore intoxications present as CNS disease. Although in light of the muscle lesions, the signs could be explained as muscular pain and weakness, we should remember that an ionophore neuropathy is observed in some toxicity trials.[5] Our ewe had no lesions in the sciatic or femoral nerves, but some conduction problems may be occurring.

JPC Diagnosis: Skeletal muscle: Degeneration and necrosis, diffuse, severe, Hampshire ewe, *Aries ovis*.

Conference Comment: As mentioned by the contributor, this case is an excellent example of extensive monophasic skeletal muscle necrosis. Classification of muscle degeneration and necrosis is based on the distribution of the lesion and the duration of the insult. Characterization of the type of skeletal muscle necrosis gives insight on the potential cause and helps narrow down the list of differential diagnoses. As a result, a classification scheme breaks muscle necrosis into four broad categories, including focal monophasic, multifocal monophasic, focal polyphasic, and multifocal polyphasic. Focal monophasic is the result of a single mechanical injury, such as intramuscular injection or focal trauma. This case is representative of the multifocal monophasic pattern, which is caused by a single massive exposure of myotoxic drugs, such as ionophores (monensin and lasalocid), or metabolic disorder.[11] Exertional capture

myopathy also produces widespread monophasic skeletal muscle necrosis with a similar histologic appearance to this case. Polyphasic reactions are the result of repeated and ongoing skeletal muscle insult occurring over a prolonged period as a result of repeated trauma (focal) or nutritional deficiencies, inflammatory myopathies, or genetic disorders (multifocal). Skeletal muscle regeneration, mineralization, and deposition of fibrous connective tissue, all key features of polyphasic necrosis, are not prominent in this case.[3,11] Nice examples of multinucleated satellite cells are scattered throughout this tissue section and represent only the beginning stages of regeneration.

pressure, trauma, or ischemia can produce global myofiber necrosis. Necrosis is commonly triggered by increased intracellular calcium concentration, often released from high levels stored in the sarcoplasmic reticulum. Initially, segmental changes are represented by myofiber hyper-contraction, and cross sections appear large and dark with hyalinization and loss of cross striations. Further insult results in sarcoplasmic fragmentation that can lead to dystrophic myofiber mineralization, often seen in chronic myopathies.[3,11]

Skeletal myofibers are classified as permanent cells and are not capable of cell

Skeletal muscle, sheep. Damaged myofibers exhibit a wide range of degenerative features: variation in fiber size myofiber swelling and hypereosinophilia; myofiber vacuolation (myofibrillolysis), an proliferation and hypertrophy of satellite nuclei. Necrotic changes contraction band formation, myofiber fragmentation and infiltration of the sarcolemma by macrophages. (HE, 200X).

Conference participants briefly reviewed the stages of skeletal muscle necrosis, re-generation, and repair. Myofibers are long and multinucleated and thus often undergo segmental necrosis rather than necrosis of the entire muscle fiber; however, extreme

division. As a result, skeletal muscle regeneration depends on the activation of satellite cells, normally resting between the sarcolemma and the basement membrane. These cells are highly resistant to injury and are activated by necrosis of adjacent myofibers.[3,11] Satellite cells begin

4

proliferation and differentiation into myoblasts in the early stages of skeletal muscle regeneration. Concurrently, macrophages migrate from the peripheral blood and phagocytose necrotic debris leaving a potential space within the damaged muscle. The initial infiltrating macrophages are of the M1 inflammatory phenotype but later switch to the M2 anti-inflammatory phenotype.[11] If the basement membrane is intact, the potential space is filled by a scaffold, called the sarcolemmal tube, which prevents the local migration of fibroblasts and instead acts as a guide for proliferating myoblasts. Within the sarcolemmal tubes, satellite cells, known as activated myoblasts at this stage, can be observed undergoing mitoses. Within hours, sarcolemmal tubes fuse end-to-end and form myotubes that eventually mature into skeletal myofibers over the course of a few days. Initial infiltrating M1 macrophages are tough to stimulate proliferation of the myoblasts, while M2 macrophages promote the formation of the myotubes.[3,11]

In contrast, if large enough numbers of satellite cells are killed and if the basement membrane is destroyed, the sarcolemmal tube is not formed, and there is no proliferation of myoblasts. This allows the influx of fibroblasts into the areas of necrosis resulting in healing by fibrosis rather than regeneration. Additionally, in cases where there is disruption of the basement membrane but satellite cells are still viable, regeneration is disorganized and ineffective due to disorganization of proliferating myotubes. This is typified by the presence of muscle giant cells (large, pleomorphic multinucleated giant myoblastic cells) and fibrous connective tissue.[3,11]

Contributing Institution:

Department of Veterinary Pathobiology
College of Veterinary Medicine
Texas A&M University
College Station, TX

References:

1. Anderson TD, Van Alstine WG, Ficken MD, Miskimins DW, Carson TL, Osweiler GD. Acute monensin toxocosis in sheep: Light and electronmicroscopic changes. *Am J Vet Res*. 1984; 45:1142-1147.
2. Bourque JG, Smart M, Wobeser G. Monensin toxicity in lambs. *Can Vet J*. 1986; 397-399.
3. Cooper BJ, Valentine BA. Muscle and tendon. In: Maxie MG ed. *Jubb, Kennedy, and Palmer's Pathology of Domestic Animals*. Vol 1. 6th ed. Philadelphia, PA: Elsevier; 2016:180-185.
4. Confer AW, Reavis DU, Panciera RJ. Light and electron microscopic changes in cardiac and skeletal muscle of sheep with experimental monensin toxicosis. *Vet Pathol*. 1983; 20:590-602.
5. Gregory DG, Vanhooser SL, Stair EL. Light and electron microscopic lesions of broiler cickens due to roxarsone and lasalocid toxicoses. *Avian Dis*. 1995; 39:408-416.
6. Horton GMJ, Stockdale PHG. Lasalocid and monensin in finishing diets for early weaned lambs with naturally occurring coccidiosis. *Am J Vet Res*. 1981; 42:433-436.
7. Jones A. Monensin toxicosis in 2 sheep flocks. *Can Vet J*. 2001; 42:135-136.
8. Mendes O, Mohamed F, Gull T, de la Concha Bermejello. Monensin poisoning in a sheep flock. *Sheep and Goat Res J*. 2003; 18: 109-113.
9. Novilla MN. The veterinary importance of the toxic syndrome induced by ionophores. *Vet and Hum*

Toxicol. 1992; 34: 66-70.

10. Nation PN, Crowe SP, Harries WN. Clinical signs and pathology of accidental monensin poisoning in sheep. Can Vet J. 1982; 23: 323-326.
11. Valentine BA. Skeletal muscle. In: McGavin MD,ed. *Pathologic basis of Veterinary Disease*. 6th ed. St. Louis, MO: Elsevier Mosby; 2017:922-926.
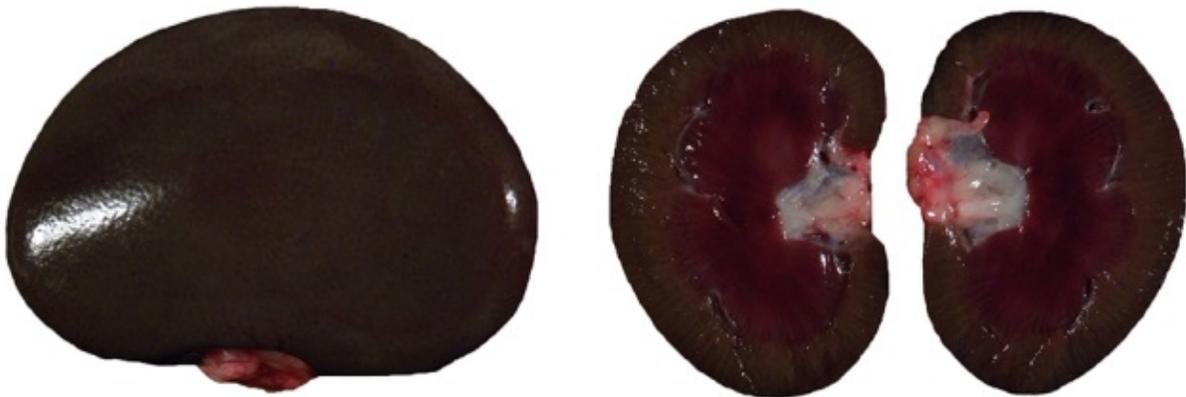
CASE II: 13A456 (JPC 4068000).

Signalment: 11-year-old male rhesus macaque (Macaca mulatta).

History: An 11-year intact male Indian origin rhesus macaque had an eight-year history of frequent intermittent vomiting. The animal was housed indoors. Over the course of eight years, this animal's therapeutic regime consisted of BSS 262-524mg/day, famotidine 3.5-5mg/day, and omeprazole 6mg/day. These medications were administered singularly or in combination. An underlying cause for the chronic emesis was not determined.

Gross Pathology: At necropsy, the animal weighed 10.3 kg and had a body condition score of 3.5/5. Significant gross findings included bilateral renal cortices that were uniformly dark green to black, with dark red medullas. The urinary bladder contained approximately 15 ml of clear, pale yellow urine. The remainder of the genitourinary system was unremarkable. Other gross findings included several diverticula in the transverse colon containing firm to inspissated black pigmented stool; the gastrointestinal tract was otherwise unremarkable.

Laboratory results: Toxic element screening, including bismuth levels, was performed on frozen kidney tissue at Michigan State University's Diagnostic Center for Population and Animal Health (Lansing, MI). Bismuth levels were 110.6 ppm. Lead levels were unremarkable at <0.50ppm.

Histopathologic Description: Light microscopy of H&E stained sections revealed numerous proximal renal tubular epithelial cells that contained a single, large, discrete, well-demarcated magenta to brown
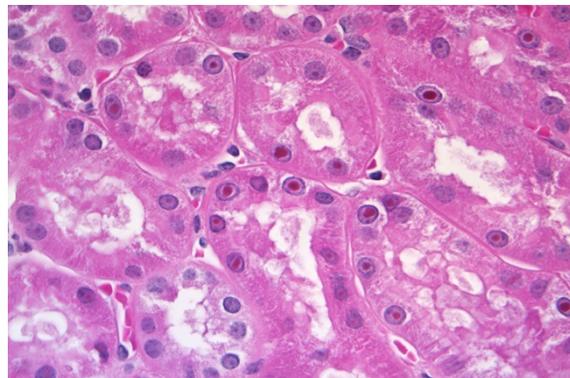

Kidney, rhesus macaque. Bilaterally, the renal cortex was uniformly dark green to black, with dark red medullas. (Photo courtesy of: Oregon National Primate Research Center, Division of Comparative Medicine and Pathology, 505 NW 185th Ave, Beaverton, OR 97006 http://www.ohsu.edu/xd/research/centers-institutes/onprc/).

intranuclear inclusion. A smaller number of tubular epithelial cells contained granular magenta to brown intracytoplasmic material. The remainder of the kidney was histologically unremarkable. The inclusions were negative when stained with Ziehl-Neelson acid fast, and appeared pale gray (negative) with Perl's Iron, blue to grey (negative) with Periodic Acid-Schiff (PAS), light brown (negative) with Alizarin red stain for calcium, and light grey (negative) with reticulin stain. In contrast, the inclusions stained black with Fontana Masson and Churukian- Schenk stains. With all these stains, the granular cytoplasmic material displayed the same staining characteristics as the intranuclear inclusions. Electron microscopy (EM) revealed numerous renal cortical tubular epithelial cells that contained a single, variably sized intranuclear inclusion. The inclusions are composed of densely grouped, co-aggregated, electron-dense crystalline material which appeared variably star or asterisk-shaped. The inclusions did not peripheralize or displace the nucleolus and the remaining nuclear structures appeared normal.

Contributor's Morphologic Diagnosis: Kidney, proximal convoluted tubules: Intranuclear pigmented inclusion bodies, marked, multifocal with mild, multifocal intracytoplasmic pigment deposition.
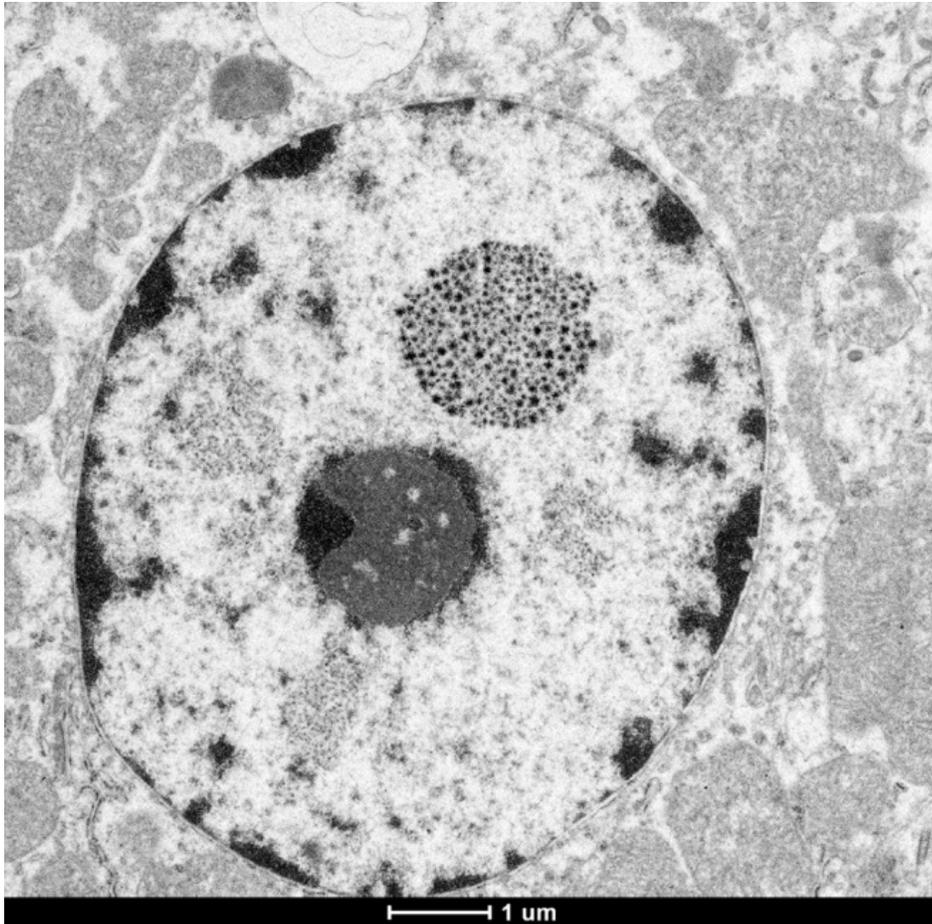
Contributor's Comment: Bismuth compounds are a rarely reported cause of both tissue pigmentation and intranuclear inclusions in man and laboratory animals. Historically, parenteral bismuth administration was used as a common treatment for syphilis. Histology of renal tissue from deceased patients routinely revealed intranuclear and intracytoplasmic bismuth deposition in epithelial cells of the convoluted tubules.[4,12] Oral bismuth

Kidney, rhesus macaque. Proximal renal tubular epithelial cells often contain a single large magenta intranuclear inclusion. (Photo courtesy of: Oregon National Primate Research Center, Division of Comparative Medicine and Pathology, 505 NW 185th Ave, Beaverton, OR 97006 http://www.ohsu.edu/xd/research/centers-institutes/onprc/). (HE, 400X)

preparations, a mainstay of treatment for diarrhea, can result in transient pigmentation of the tongue and fecal material within the colon through reaction of bismuth salts with hydrogen sulfide produced in the oral cavity or within the colon, creating an insoluble black salt.[2]

Bismuth subsalicylate (BSS) is the primary ingredient in Pepto-Bismol (Proctor & Gamble, USA). It is estimated that roughly 99% of bismuth ingested is excreted in the feces.[2] Bismuth levels in blood increase with chronic administration, but are not routinely associated with toxicity.[2] Despite the low levels of bismuth absorbed and the minimal risk of toxicity, the literature discourages prolonged administration.[2] The absorption of bismuth from the gastrointestinal tract may be increased under a variety of situations including patient variation, the formulation of the bismuth compound or salt, time of gastric emptying, alteration of gastric pH, and co-administration of bismuth with products or foodstuffs that contain thiol groups, cysteine, and/or fruit juice.[1-7, 11] Bismuth is deposited in multiple organs, but is preferentially retained longer in the

Kidney, rhesus macaque. Ultrastructurally, nuclei of proximal convoluted tubules contain one or multiple intranuclear inclusions which appear to be a composite of asterisk-shaped crystalline material. (Photo courtesy of: Oregon National Primate Research Center, Division of Comparative Medicine and Pathology, 505 NW 185th Ave, Beaverton, OR 97006 http://www.ohsu.edu/xd/research/centers-institutes/onprc/).

higher than normal acceptable bismuth levels. Based on literature published in wild game birds normal levels of bismuth in liver and muscle are <0.1ppm.[5] Work performed in rats suggests that normal tissue levels for bismuth in kidneys are <0.2 ppm.[1] The heavy metal screening also revealed levels of lead considered within normal limits disproving lead as the source of the intra-nuclear inclusions.

The dark green to black renal cortical pigmentation is consistent with pigmented bismuth compound accumulation. As the kidney is the documented primary target organ for bismuth accumulation, this was the most likely organ to exhibit pigmentation.[10] There was no gross or histologic evidence of this pigment in any other organs. Other causes of grossly visible green black renal pigment such as hemozoin and melanin were disproved through microscopic appearance of intranuclear localization and patient history. The animal had lived in a non-endemic area for malaria-causing Plasmodium sp. throughout its lifetime and the animal had not received any blood or tissue transplants that could have resulted in iatrogenic transmission. Further, there was no histologic evidence of malaria, effectively ruling out hemozoin pigment.

kidney when compared to other organs.[10] Renal bismuth inclusions have been identified 1-30 years after parenteral treatment.[10]

The diagnosis of gross renal bismuth pigmentation and intranuclear bismuth inclusions in this macaque was based on the combination of a history of chronic BSS administration, elemental screening, gross and histologic findings, histochemical stain results, and electron microscopy.
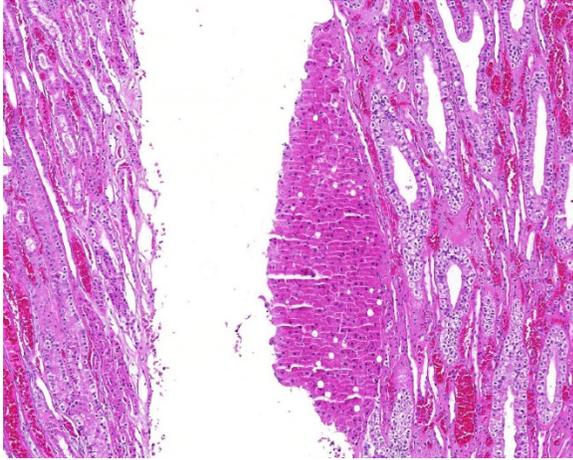
Toxic element screening confirmed not only the presence of bismuth (110.6ppm), but that the levels were measured at 500-1000 times

Kidney, rhesus monkey. A choristoma of hepatocytes is present within the renal medulla. (HE, 88)

A variety of histochemical stains were employed to help correlate the appearance of the intranuclear inclusions and intra-cytoplasmic granules observed in the renal tubular epithelium with the elemental screening results. Ziehl-Neelson acid fast stain is used primarily for the detection of acid-fast bacteria. However, lead inclusions are known to stain positive on paraffin embedded tissue, but less intensely when compared to fresh non-paraffin embedded samples.[12] Compared to bismuth inclusions that stain acid-fast positive with frozen tissue and negative with paraffin embedded tissues.[3] Perl's Iron stain used to detect ferric iron in tissue was negative, determining that iron and iron-containing compounds such as ferritin were not present. Alizarin Red stain for calcium was also negative. To demonstrate that the material was intrinsically pigmented, unstained tissues were examined revealing brown inclusions. When unstained tissue sections were treated with a 10 second application of 30% hydrogen peroxide, the inclusions were no longer visible. The presumptive mechanism for decolorization with hydrogen peroxide is that the hydrogen peroxide oxidizes the bismuth sulfide resulting in formation of colorless bismuth sulfate.[13] Melanin is resistant to decolorization with this short term hydrogen peroxide application.[13] Fontana Masson and Churukian-Schenk, silver based stains used for the non-specific demonstration of melanin and argyrophilic granules, stained the inclusions brown-black. As the hydrogen peroxide treatment suggested that the material was not actually melanin, it was presumed that the bismuth salt inclusions possessed the ability to bind silver from a silver solution and reduce it to visible metallic silver with and without a reducing agent thus exhibiting both argentaffin and argyrophilic properties.

Electron microscopy confirmed the presence of an electron dense material consistent with heavy metal or mineral within the nucleus of proximal renal tubule epithelial cells. The appearance of bismuth inclusions are dependent upon the method of fixation, sections fixed with glutaraldehyde exhibit a homogenous electron dense appearance.[4] However, inclusions in tissue fixed with osmium have a more granular and fibrillar appearance.[4] The latter is more consistent with the inclusions we identified in our osmium fixed samples.
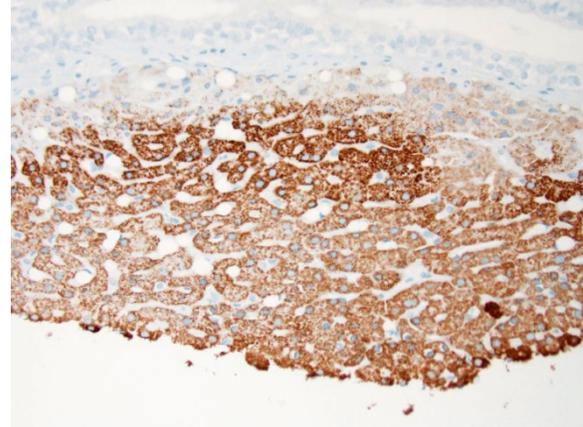
Increased absorption of bismuth in this macaque is thought to be related to a variety of factors including chronic vomiting that likely altered the time of gastric emptying. Additionally, concomitant therapeutics, famotidine and omeprazole, were frequently administered with the primary therapeutic BSS for this animal's gastrointestinal disturbance. Famotidine is an H2 receptor antagonist. Work performed with other H2 receptor antagonists (ranitidine) has demonstrated an increased systemic absorption of tripotassium dicitrate bismuthate.[8] Omeprazole, a proton pump inhibitor has also been linked to increased

absorption of tripotassium dicitrate bismuthate.[11] Although this animal was administered BSS, not tripotassium dicitrate bismuthate, this still suggests an additional potential for increased absorption. Furthermore, this animal's diet of routine monkey chow contains normal dietary levels of cysteine, and as enrichment this animal routinely received whole fruits and fruit juices. Both cysteine because of its thiol group, and ascorbic acid derived from fruits and fruit juices have been linked to the formation of soluble bismuth in vivo and in vitro.[7,10] The prolonged administration of BSS by itself or in conjunction with drugs that alter gastric pH, and routine administration of foodstuffs that contain thiol group compounds and ascorbic acid could have singly or in combination been responsible for increased systemic absorption of bismuth and consequently this animal's gross and histologic findings.

JPC Diagnosis: Kidney, tubular epithelium: Intranuclear inclusions, multifocal, rhesus macaque, Macaca mulatta.

Conference Comment: We thank the contributor for their institutions' complete clinical workup and thorough review of bismuth subsalicylate (BSS) inclusions in a rhesus macaque with chronic intermittent vomiting. In this case, the inclusions are primarily localized to the proximal convoluted tubules, but they are also rarely present within the renal distal convoluted tubules and collecting ducts. No inclusions are observed within the glomeruli or vessels. While BSS has been reported to cause nephrotoxicity in other species, the inclusions within the renal tubules in this case are not associated with a lesion, indicating that these inclusions are likely incidental rather than contributing to this animal's clinical disease. As mentioned by the contributor, increased uptake of bismuth

is thought to be secondary to a number of

Kidney, rhesus monkey. Cells within the medullary choristoma stain strongly and intracytoplasmically positive for hepatocellular paraffin antibody 1. (anti-hepatocyte specific antigen, (110X)

factors, such as chronic vomiting altering gastric emptying time, and concurrent administration of famotidine and omeprazole, which all increase systemic absorption of orally administered BSS.[6,12] Conference participants briefly discussed other causes of intranuclear inclusion bodies, which included viral etiologies such as herpesviruses, adenovirus, and polyomavirus; other heavy metals, such as lead; and cytoplasmic invaginations. Likely due to the recent publication of this case in Veterinary Pathology, virtually every conference participant included BSS near the top of their list of differentials diagnoses for this lesion.[6]

In addition to the intranuclear inclusions predominantly within the renal proximal convoluted tubules, the more perceptive conference participants also identified what appeared to be a 3 x 2 mm section of liver attached to the kidney near the renal pelvis. This small section of tissue demonstrated intense and specific intracytoplasmic immunoreactivity for hepatocyte antigen run by the Joint Pathology Center after the conference. Conference participants could not reach a consensus on whether this

represented ectopic liver tissue (hepatic choristoma) or is simply a piece of liver that was dragged in during tissue processing. The tissue appears to be attached to the underlying renal parenchyma, but it is also present on a cut border, further adding to the disagreement. Hepatic choristomas have been typically reported as incidental findings in the kidney and various abdominal and extra-abdominal sites, with the gallbladder the most common location in humans. Other rare sites include the retroperitoneum and the adrenal gland. Ectopic liver has also been very rarely associated with the development of hepatocellular carcinoma.[8] If this case represents a true hepatic choristoma in the kidney, it is of academic interest, but likely of no clinical significance to this animal.

Contributing Institution:
Oregon National Primate Research Center
Division of Comparative Medicine
Beaverton, OR
http://www.ohsu.edu/xd/research/centers-institutes/onprc/

References:

1. Allain P, Krari N, Chaleil D, et al. Effects of some chelating agents on bismuth absorption in the rat. Fundam Clin Pharmacol. 1991;5(1):39-45.
2. Bierer DW. Bismuth subsalicylate: history, chemistry, and safety. Rev Infect Dis. 1990;12(Suppl 1):3-8.
3. Burr RE, Gotto AM, Beaver DL. Isolation and analysis of renal bismuth inclusions. Toxicol Appl Pharmacol. 1965;7(4):588-91.
4. Ghadially FN, Young NK. Ultrastructural and x-ray analytical studies on intranuclear bismuth inclusions. Virchows Arch B Cell Pathol. 1976;(1):45-55.
5. Jayasinghe R, Tsuji LJ, Gough WA, et al. Determining the background levels of bismuth in tissues of wild game birds: A first step in addressing the environmental consequences of using bismuth shotshells. Environ Pollut. 2004;132(1):13-20.
6. Johnson AL, Blaine ET, Lewis AD. Renal pigmentation due to chronic bismuth administration in a rhesus macaque (Macaca mulatta). Vet Path. 2015; 52(3):576-579.
7. Mahony DE, Woods A, Eelman MD, et al. Interaction of bismuth subsalicylate with fruit juices, ascorbic acid, and thiol-containing substrates to produce soluble bismuth products active against Clostridium difficile. Antimicrob Agents Chemother. 2005;49(1):431-3.
8. Merve A, Scheimberg I. Ectopic liver tissue in the kidney: Case report and literature review. Pediatr Dev Pathol. 2014; 17(5):382-385.
9. Nwokolo CU, Prewett EJ, Sawyerr AM, et al. The effect of histamine H2-receptor blockade on bismuth absorption from three ulcer-healing compounds. Gastroenterology. 1991;101(4):889-94.
10. Slikkerveer A, de Wolff FA. Pharmacokinetics and toxicity of bismuth compounds. Med Toxicol Adverse Drug Exp. 1989; 4(5):303-23.
11. Treiber G, Walker S, Klotz U. Omeprazole-induced increase in the absorption of bismuth from tripotassium dicitrato bismuthate. Clin Pharmacol Ther. 1994;55(5):486-91.
12. Wachstein M. Studies on inclusion bodies; acid-fastness of nuclear inclusion bodies that are induced by
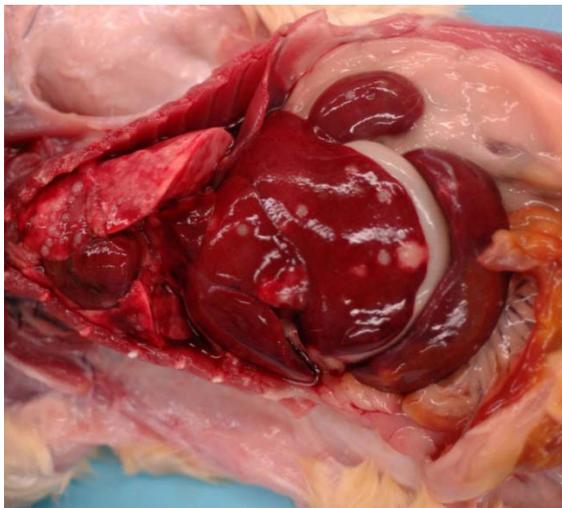
ingestion of lead and bismuth. Am J Clin Pathol. 1949;19(7):608-14.

13. Wachstein M, Zak FG. Bismuth Pigmentation: Its Histochemical Identification. Am J Pathol. 1946 May;22(3):603-11.
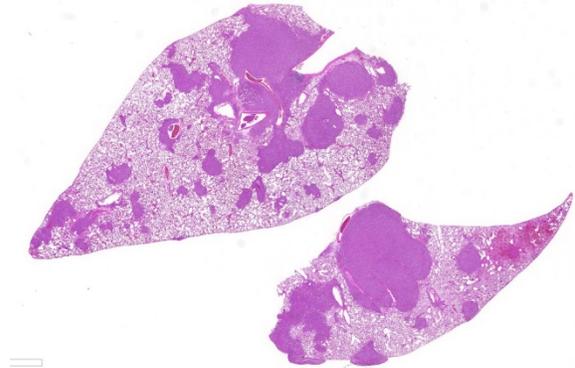
CASE III: 1519 (JPC 4084474).

Signalment: >20-month-old male Sprague-Dawley rat (*Rattus norvegicus*).

History: The rat had 4ET telemetry device implantation surgery on 28 October 2014 & was exposed to test article on 8 December 2014. The rat had two routine battery exchange surgeries on 24 February 2015 and 22 July 2015. Post-op recovery was uneventful. In early September 2015, the rat developed fluid-filled distention on both flanks. Veterinary staff attempted to manually drain several times, but size remained the same. On 10 Sept 2015, a veterinarian performed a battery exchange. During the surgery, the surgeon removed fibrous/sac-like tissues (submitted for biopsy) from both sides while draining a
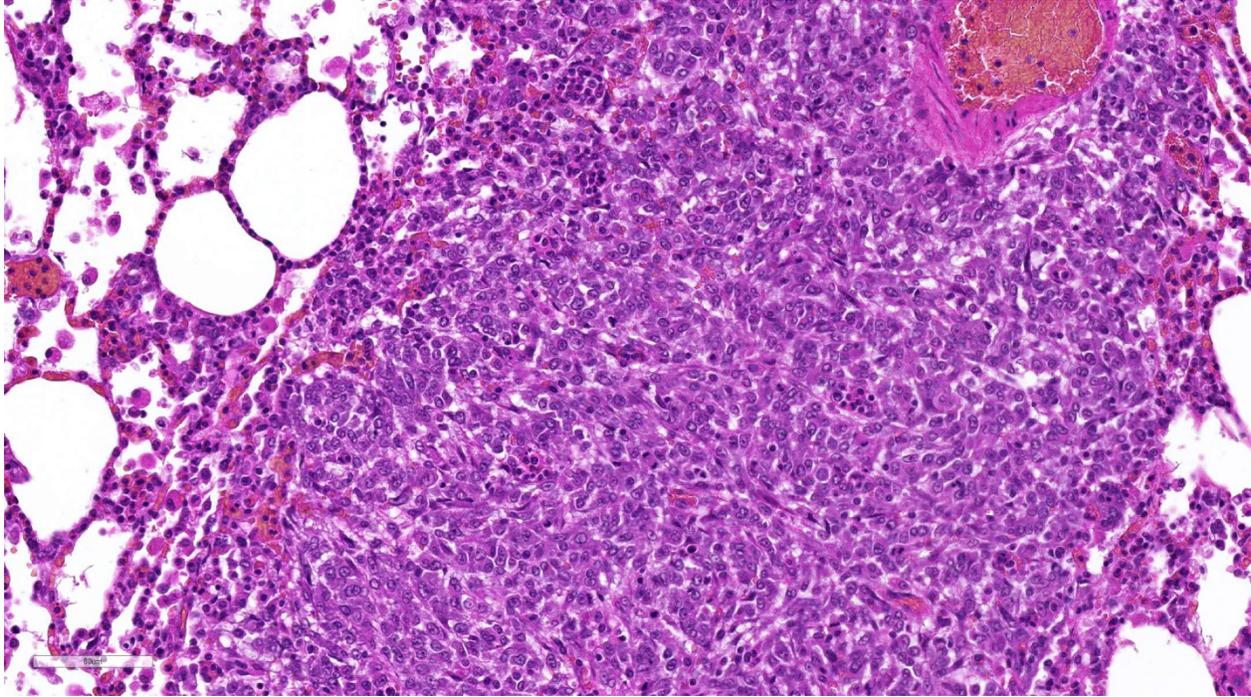

Viscera, Sprague-Dawley rat: White, firm, elevated nodules are present in the lungs, liver, spleen, and kidney.

Lung, Sprague-Dawley rat: Numerous densely cellular neoplastic nodules surround vessels and occasionally elevate the pleura. (HE 5X)

copious amount of serosanguineous fluids (no purulent fluid noted). The rat was placed on enrofloxacin (1mg/kg) post-surgery. On 23 September 2015, chlorhexidine scrub & triple antibiotic ointment treatment was started because the area at the incision site appeared raw. The rat appeared bright, alert, and responsive during rounds on 25 Sept 2015, but was found dead in the cage on the morning of 27 September 2015.

Gross Pathology: This 689 g, male, CD rat is in optimum body condition with abundant SQ & visceral fat, 3/5 BCS, & moderate autolysis, especially the GI tract. The lungs are noncollapsed & pink with multifocal dark red areas & numerous 0.2-0.4 cm, pale, soft, smooth, round, well-demarcated masses affecting all lobes. The liver has numerous 0.2-0.6 cm, pale, soft, smooth, round, well-demarcated masses extending into the parenchyma & affecting all lobes. The spleen is 6.5 x 1.5 x 0.5 cm & has a focal, 0.4 x 0.4 x 0.2 cm, pale, soft, smooth, round, well-demarcated mass. The pancreas appears nodular & firm. The left kidney has a central, approximately 0.3 x 0.3 cm, slightly raised, pale area that is wedge-shaped extending into the cortex on cut surface. The right kidney has 2 similar areas on the caudal pole. The mediastinal & perirenal lymph nodes are greenish-yellow & enlarged. The urinary bladder is empty.
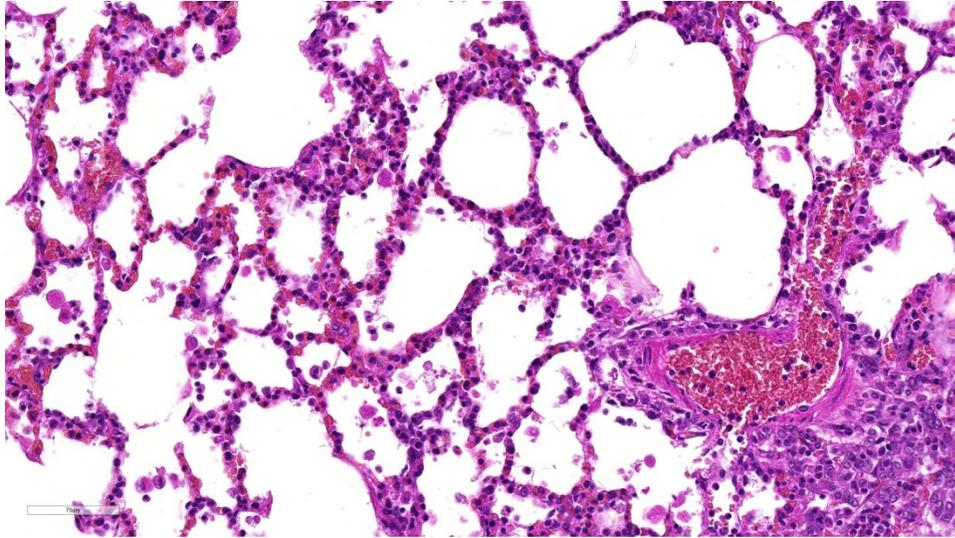
Lung, Sprague-Dawley rat: Neoplastic cells fill alveoli and efface alveolar architecture. They are spindled with indistinct cell borders and moderate amounts of a finely vacuolated cytoplasm. Aggregates of immature hematopoietic cells are scattered through the nodules. (HE 5X)

Laboratory results: None

Histopathologic Description: Lung: Multifocally invading and replacing alveoli, surrounding blood vessels and rarely filling and replacing bronchioles is an un-encapsulated, poorly demarcated, cellular neoplasm compose of either round cells arranged in sheets or less commonly palisading spindle cells all supported by a preexisting fibrovascular stroma. Neoplastic cells have indistinct cell borders, abundant pale, eosinophilic cytoplasm, round, oval or reniform nucleus with vesiculate chromatin and distinct nucleolus. Mitotic rate is 2 per HPF. Multifocally neoplastic cells are expanding pleura, filling or expanding alveolar septa and filling blood vessels. Within less affected areas, alveoli often contain fibrin, hemorrhage, cellular debris and small to moderate numbers of neutrophils, lymphocytes, and alveolar macrophages. Multifocally individual alveoli contain small clusters of neoplastic cells. Focally a large bronchiole is filled with fibrin/cellular debris/mucus admixed with few lymphocytes, macrophages and sloughed mucosal epithelial cells.

Contributor's Morphologic Diagnosis: Lung: Malignant neoplasm, favor histiocytic sarcoma.

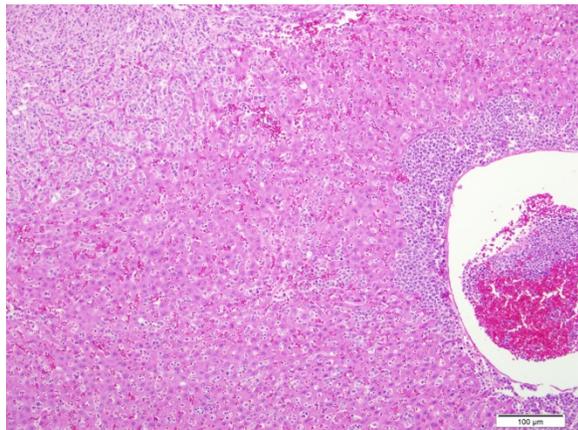**JPC Diagnosis:** 1. Lung: Histiocytic sarcoma, Sprague-Dawley rat, *Rattus norvegicus*.

2. Lung: Pneumonia, interstitial, necrotizing, fibrinonecrotic and eosinophilic, multifocal, moderate with vascular necrosis.

Lung, Sprague-Dawley rat. A diffuse interstitial pneumonia, characterized by thickened hypercellular alveolar septa, mild type II pneumocyte hyperplasia, and fibrin within alveoli is present. No previous manipulation of this animal was noted in the submitted history. (HE, 280X)

Contributor's Comment: Histiocytic sarcoma in rats is the most common nonlymphoid hematopoietic neoplasm.[6] The incidence in Sprague-Dawleys has been reported to be as low as 1%[6] and as high as 4.7%[8] with no sex predilection. The occurrence of this neoplasm is seen in animals >12 months of age with one study showing over 50% of cases in animals in a 18-23 month age group.[7] At necropsy, sarcomas of this type may be present in the liver, lymph nodes, lung, spleen, mediastinum, retroperitoneum, or sub-cutaneous tissue.[1] The most common localizations of this tumor are different between rat strains and are as follows: the liver and lungs in Sprague-Dawley rats, liver, bone marrow, lymph nodes, spleen and lungs in Fischer and Donryu rats and subcutis in Wistar rats.[6] In our case, neoplastic cells were also seen in the kidney, pancreas, adipose tissue surrounding a number of the listed organs above as well as within vascular spaces.

Conference Comment:

Histiocytic sarcoma (HS) is a relatively common neoplasm in aging Sprague-Dawley rats, but they have also been reported much less commonly in other strains (Wistar, Fischer 344, Osborne-Mendels).[1,6,7] Grossly, the neoplasm is typically pale white to tan, homogenous, and firm forming variably sized masses that infiltrate and efface normal tissue architecture. HS can develop at multiple locations, but primary sites are most often in the liver, lymph nodes, lungs, spleen, bone marrow, retroperitoneum, and the subcutis.[1,6,7,9] Metastatic sites can include any organ, but are most commonly present in the liver, kidneys, draining lymph node, and lungs.[9] Histologically, HS have a variable appearance of sheets of large pleomorphic and anaplastic cells with abundant vacuolated cytoplasm and Langhans-type multinucleated giant cells or interlacing bundles and streams of elongate palisading fusiform spindle cells, which is the predominant feature of this case.[1,9]

Although not mentioned by the contributor as a component of this case, conference participants discussed the frequent association of HS with hyaline droplet (HD) accumulation in the renal proximal convoluted tubules. In these cases, the hyaline droplets are immunopositive for lysozyme, a major protein secreted by macrophages and monocytes.[2-5] There is a direct qualitative correlation between a droplet accumulation in the kidney and increased tumor burden in rats. In cases where the HS is confined to a single location, there may be little to no hyaline droplet accumulation. The widespread metastatic disease and high tumor burden, described by the contributor, suggests that

Liver, Sprague-Dawley rat. Neoplastic cells (upper left and adjacent to the vessel at right) are present within the liver. (HE, 100X)

there is renal tubule hyaline droplet in this case.[2-5] HD can also occur in response to a number of other pathologic conditions associated with accumulation of alpha-2u-globulin in the male rat. These droplets form in the P2 segment of the proximal tubule and represent secondary lysosomes containing alpha-2u-globulin bound to a variety of chemicals, including volatile hydrocarbons, d-limonene, unleaded gasoline, tetra-chloroethylene, 1,3,5-trinitrobenzene, diethylacetylurea, and sodium barbital.[2-5] They have also been observed in chronic progressive nephropathy of rats associated with accumulation of albumin.[2,4] The HD seen in tumor-bearing rats are histologically indistinguishable from rats with alpha-2u-globulin nephropathy. As mentioned above, HD secondary to HS will be strongly immunopositive for lysozyme, but immunonegative for alpha-2u-globulin staining; the reverse is true for alpha-2u-globulin nephropathy.[2-5]

In addition to multifocal infiltration of HS within this section of lung, conference participants also noted a moderate infiltration of alveolar macrophages and eosinophils, predominantly infiltrating multifocal areas of alveolar septal thickening and necrosis. Accumulation of inflammatory cells is not uncommon in pulmonary neoplastic disease, especially HS[9]; however, conference participants could not explain the widespread presence of eosinophils within areas of inflammation and necrosis. It is possible that the inflammation present in this case may be related to the administration of the test article rather than the neoplasm; although, the nature of the test article is not specified by the contributor.

Contributing Institution:

References:

1. Barthold SW, Griffey SM, Percy DH. Rat. In: *Pathology of laboratory rodents and rabbits*. 4th ed. Ames, IA: John Wiley & Sons, Inc.; 2016:167.
2. De Rijk EPCT, Ravesloot WM, et al. A fast histochemical staining method to identify hyaline droplets in the rat kidney. *Toxicol Pathol*. 2003; 31:462-464.
3. Frith CH, Ward JM, and Chandra M. The morphology, immunohistochemistry, and incidence of hematopoietic

neoplasms in mice and rats. *Toxicol Pathol*. 193; 21:06–218. 1993.

4. Hard GC. Some aids to histological recognition of hyaline droplet nephropathy in ninety-day toxicity studies. *Toxicol Pathol*. 2008; 36:1014-1017.
5. Hard GC, Snowden RT. Hyaline droplet accumulation in rodent kidney proximal tubules: An association with histiocytic sarcoma. *Toxicol Pathol*. 1991; 19:88-99.
6. Kemmochi Y, Takahashi A, Miyajima K, Yasui Y, Tanoue G, Shoda T, Kakimoto K. Spontaneous histiocytic sarcoma of the popliteal lymph node in a young Sprague-Dawley rat. *J Toxicol Pathol*. 2010; 23:161-164.
7. Ogasawara H, Mitsumori K, Onodera H, Imazawa T, Shibutani M, and Takahashi M. Spontaneous histiocytic sarcoma with possible origin from the bone marrow and lymph node in Donryu and F-344 rats. *Toxicol Pathol*. 1993; 21:63–70.
8. Squire RA, Brinkhous KM, Peiper SC, Firminger HI, Mann RB, and Strandberg JD. Histiocytic sarcoma with a granuloma-like component occurring in a large colony of Sprague-Dawley rats. *Am J Pathol*. 1981; 105: 21–30.
9. Valli VEO, Kiupel M, Bienzle D. Hematopoeitic system. In Maxie MG, ed. *Jubb, Kennedy and Palmer's Pathology of Domestic Animals*. Vol 3. 6th ed. Philadelphia, PA: Elsevier Ltd; 2016:250-255.
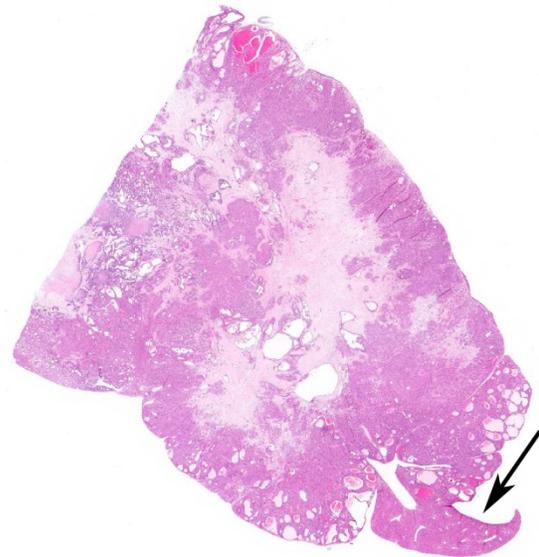
CASE IV: 0601909 (JPC 4089360).

Signalment: Two-year-old male B6C3F1 mouse (*Mus musculus*).
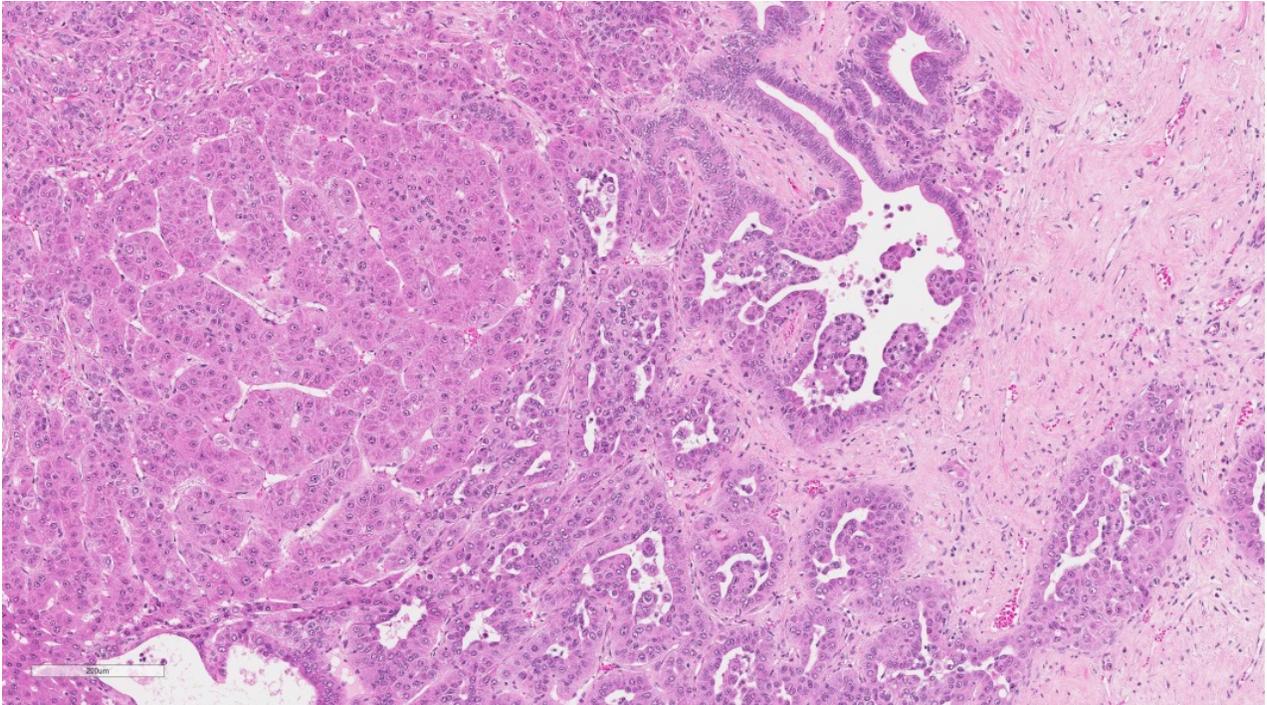
History: This mouse was in the control group of a two-year study investigating the carcinogenicity of kava kava extract. It was sacrificed on Test Day 668, due to moribund condition. Clinical observations included ruffled fur, lethargy and thin body condition.

Gross Pathology: Gross lesions described at necropsy included: a single tan mass, approximately 27x17x12 mm, on the left lateral liver lobe; and several white nodules, up to 5 mm diameter, on the visceral pleura, lungs, and mediastinum.

Laboratory results: None

Liver, B6C3F1 mouse. 95% of the submitted section of liver is effaced by a multilobular, occasionally cystic neoplasm with large central areas of necrosis (normal liver at lower right.) (HE, 5X)

Liver, B6C3F1 mouse. Neoplastic cells differentiate along multiple phenotypic lines, with large plates of neoplastic cells resembling hepatocytes at left, and neoplastic cells recapitulating bile ducts with a single layer of columnar epithelium lining cystic spaces and forming micropapillary projections at right. (HE, 136X)

Histopathologic Description: Most of this section of liver lobe is replaced by a large mass extending to the capsular surface. The mass is composed of irregular acini and variably-sized cystic spaces interspersed with more densely cellular areas and areas of fibrosis or necrosis. Acini are lined by columnar epithelium with prominent hyper-chromatic nuclei and scant cytoplasm. More densely cellular areas are comprised of hepatocytes with a central vesicular nucleus containing 1 or 2 prominent nucleoli, and abundant cytoplasm. These cells are arranged in packets, in trabeculae more than 3 cells thick, or around cystic spaces. The cystic spaces are lined by one or more layers of flattened to plump hepatocytes, with occasional papillary projections extending into the lumens; lumens often contain sloughed epithelial cells, lightly stained fibrillar eosinophilic material, and occasional extravasated erythrocytes. In other areas, densely-packed, small round to elongated cells with hyperchromatic nuclei form a sarcomatous pattern, often extending into areas of fibrosis. Occasional endothelial-lined spaces contain erythrocytes, small clusters of white blood cells (mainly neutrophils) and single or clusters of neoplastic cells.

Contributor's Morphologic Diagnosis:
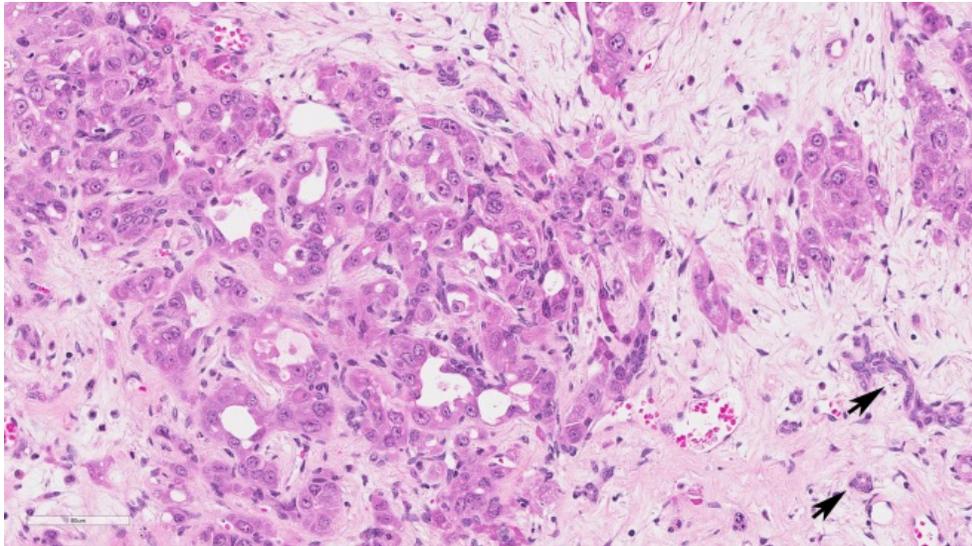Liver – Hepatocholangiocarcinoma
Tissue not included:
Lung – Hepatocholangiocarcinoma, metasta-tic
Lymph node, mediastinal – Hepatocholan-giocarcinoma, metastatic
Thymus – Hepatocholangiocarcinoma, metastatic
Heart, pericardium – Hepatocholangio-carcinoma, metastatic

Contributor's Comment: This hepato-cholangiocarcinoma (HCCC) typically contains both malignant hepatocellular and malignant biliary components, as well as foci of markedly undifferentiated sarcoma-

Liver, B6C3F1 mouse. Centrally, neoplastic cells formed well-differentiated neoplastic bile ducts on a dense fibrous stroma. A few pre-existent biliary ductules are present at lower right (arrows.) (HE, 168X)

have many characteristics of malignancy, such as frequent mitoses, nuclear pleo-morphism, local invasion, and widespread metastasis.[4,6,7] HCCC often contains large cystic or necrotic areas within the central portions of the neoplasm, as demonstrated in this case. Additionally, there are occasional ducts within the neoplasm, lined by both hepatocytic and biliary epithelial cells, in conjunction with multifocal areas of poorly differentiated mesenchymal spindloid cells arranged in short interlacing streams and bundles. Proliferation of sarcomatous cells is a

like cells, as described in a poster presented by the National Institute of Environmental Health Sciences (NIEHS) and Experimental Pathology Laboratories, Inc. (EPL).[4] HCCC is rarely reported in mice and rats. However, it has been induced by some chemicals tested in the National Toxicology Program (NTP) studies.[2,4] It is an aggressive neoplasm that metastasizes readily.
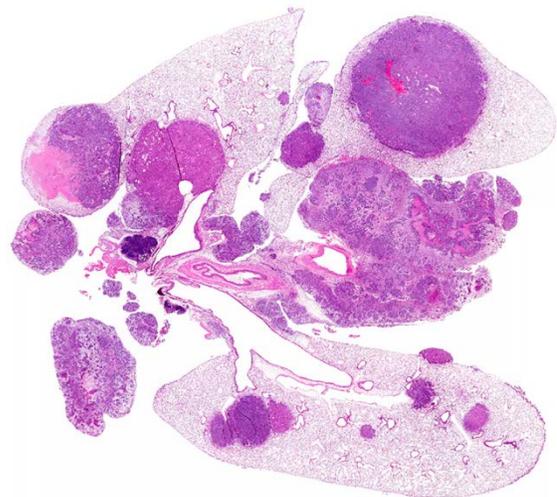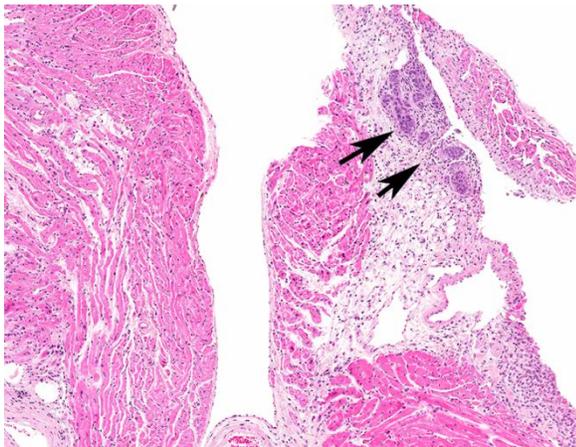
JPC Diagnosis: Liver: Hepato-cholangiocarcinoma, B6C3F1 mouse, *Mus musculus*.

Conference Comment: Hepato-cholangiocarcinoma (HCCC) is a rare spontaneous neoplasm with an incidence of less than 0.5% in B6C3F1 mice, according to the National Toxicology Program (NTP) database.[4,6] HCCC is a primary liver neoplasm comprised of both neoplastic hepatocytes and neoplastic bile duct epithelial cells.[4,6] The biliary component forms tubules and acini or small nests, while the hepatocellular component forms trabeculae, glands, or solidly cellular areas of neoplastic cells. Both neoplastic hepatocytes and bile duct epithelial cells

Lung, B6C3F1 mouse. All lung lobes contain metastatic nodules. (HE, 0.7X) (Photo courtesy of: Experimental Pathology Laboratories, Inc., P.O. Box 12766, RTP, NC 27709, www.epl-inc.com).

frequently reported feature of this malignant neoplasm.[6,7] In previously studies, 84% of mice with HCCC had metastasis to multiple tissues, similar to what is reported by the contributor here.[6] The histo-morphologic variability of this neoplasm and widespread metastasis may pose a diagnostic challenge in determining the site of origin. Metastatic lesions may contain only one of the three neoplastic populations mentioned above, further confounding the diagnosis.[6]

Mediastinum, B6C3F1 mouse. Neoplastic nodules are also present within the mediastinum at the heart base. (HE, 10X) (Photo courtesy of: Experimental Pathology Laboratories, Inc., P.O. Box 12766, RTP, NC 27709, www.epl-inc.com).

As mentioned previously, spontaneous occurrence of HCCC is exceedingly rare in mice; however, malignant transformation has been experimentally associated with chemical carcinogens, such as trimethylolpropane tricrylate, benzidine dihydrochloride, and N-2-acetylaminofluorene.[4] The B6C3F1mouse is a hybrid strain that is the result of a cross between a male C3H and a female C57BL/6 mouse. This relatively hardy mouse strain has been used by the NTP for decades as part of carcinogenesis, toxicity, and transplant studies.[2]

Contributing Institution:
Experimental Pathology Laboratories, Inc.

Research Triangle Park, NC
http://www.epl-inc.com

References:

1. Adams ET, Auerbach S, Blackshear PE et al. Proceeding of the 2010 National Toxicology Program satellite symposium. *Toxicol Pathol*. 2010; 39:240-246.
2. Gad SC, Clifford C, Goodman D. The mouse. In Gad SC ed. *Animal Models in Toxicology*. 3rd ed. Boca Raton, FL: CRC Press; 2016:76-78.
3. Hailey JR, Nold JB, Brown RH et al. Biliary proliferative lesions in the Sprague-Dawley rat: Adverse/non-adverse. *Toxicol Pathol*. 2014; 42:844-854.
4. Harada T, Enomoto A, Boorman GA, Maronpot RR. Liver and gallbladder. In: Maronpot RR, Boorman GA, Gaul BW eds. *Pathology of the Mouse*. Vienna, IL: Cache River Press; 1999:153.
5. Maronpot RR. Rodent Liver - Neoplastic. 2015. http://focusontoxpath.com/rodent-liver-lesions-neoplastic/
6. Moore R,Willson G, Miller R, Malarkey D, Kissling et al. Hepatocholangiocarcinomas in B6C3F1 Mice in National Toxicology Program (NTP) Studies.
7. Thoolen B, Maronpot RR, Harada T et al. Proliferative and nonproliferative lesions of the rat and mouse hepatobiliary system. *Toxicol Pathol*. 2011; 38:5S-81S.